We are IntechOpen, the world's leading publisher of Open Access books Built by scientists, for scientists

6,900
Open access books available

186,000
International authors and editors

200M
Downloads

154
Countries delivered to

Our authors are among the

TOP 1%
most cited scientists

12.2%
Contributors from top 500 universities

CLARIVATE ANALYTICS
BOOK CITATION INDEX
INDEXED

WEB OF SCIENCE™

Selection of our books indexed in the Book Citation Index
in Web of Science™ Core Collection (BKCI)

Interested in publishing with us?
Contact book.department@intechopen.com

Numbers displayed above are based on latest data collected.
For more information visit www.intechopen.com

Improvement of Efficiency of Dye Sensitized Solar Cells by Incorporating Carbon Nanotubes

Md. Mosharraf Hossain Bhuiyan, Fahmid Kabir,
Md. Serajum Manir, Md. Saifur Rahaman, Prosenjit Barua,
Bikrom Ghosh, Fumiaki Mitsugi and Tomoaki Ikegami

Abstract

Dye-sensitized solar cells (DSSCs) have aroused intense attention over the past three decades owing to their low cost, inexpensive raw materials, simple fabrication process, and employment of eco-friendly materials. Recently, to take advantage of their lower electrical resistance, excellent electrocatalytic operation, mechanical integrity, low cost, and flexibility, carbon nanotubes CNTs have been incorporated into DSSCs with a view to improve the efficiency further. CNT can be used in the anode, electrolyte, and counter electrode. The incorporation of CNTs into the anode's semiconductor material decreases the host material's resistance and increases thermal conductivity, electrical conductivity, mechanical strength, and durability. CNTs in ionic liquids have been investigated as a potential alternative for traditional liquid electrolytes for DSSC application because of low viscosity, low vapor pressure, high diffusion coefficient, high electrochemical, and thermal stability. CNT based counter electrode has attracted considerable interest because of its fast electron transfer kinetics and large surface area. This book chapter provides an insight into the fabrication of DSSCs by incorporating CNT and its effects on cell conversion efficiencies.

Keywords: dye sensitized solar cell, carbon nanotubes, efficiency

1. Introduction

In recent years, world energy consumption has increased significantly due to rapid global population growth, improved quality of life, and new technologies. United States Department of Energy (USDoE) anticipates that global energy demand will double by 2050 and triple by 2100 [1]. About 87% of energy demands are supplied by burning fossil fuels, such as coal, oil, and natural gases [2]. However, it has become a major concern about the environmental damage caused by the combustion method. Excessive use of fossil fuel energy sources urges researchers to think about the alternatives to eternal clean energy sources. The use of renewable energy is of great significance due to the rising cost of fossil fuels in tandem with a decrease in carbon dioxide emissions that avoids global warming. Significant

improvements have been made in this regard, including energy technologies focused on wind power, biofuels, solar panels, and fuel cells [3, 4].

Solar energy will effectively meet some of the energy needs of future generations. The $3x10^{24}$ Joule/year supply of energy from the sun to the earth is 10 000 times more than the global energy requirement. This suggests that the use of 10% efficient photovoltaic cells will cover just 0.1% of the earth's surface area that could supply our current electricity needs [5]. In addition to photovoltaic device technologies, protect the global environment, and ensure economic growth with sustainable resources [6]. A solar cell or photovoltaic device is a solid-state device that is generally used for converting solar energy into useable electricity. The main advantage of the solar cells is that it does not require fossil fuel burning and does not produce any harmful emission [2]. The development of solar cells can be divided into three generations: First generation, second generation, and third generation solar cell. First generation or crystalline-silicon based solar cell has high cell efficiency($\sim$26.7% against theoretical limit $\sim$29%), which dominates the global solar cell market ($\sim$90%) [7]. However, the rigid cell structure and high cost related to manufacturing silicon wafers limit the use of first generationsilicon-based solar cells. Second generation or thin-film solar cell is fabricated by depositing multiple layers of photovoltaic material on plastic, glass, or metal substrate. Thin-film solar cell thickness can vary from few nanometers to 10 microns. However, Indium and Tellurium's scarcity makes it somewhat difficult to commercializeand large-scale production of the thin-film solar cell. Also, cadmium is a highly toxic material, which poses both severe health and environmental hazards. Third-generation solar cells are targeted to achieve both high efficiency and low cost. The theoretical cell conversion efficiency of third-generation solar cells varies from 31 to 41%, and it is expected that this limit can be easily overcome by using semiconductor nanoparticles [8]. Perovskite solar cell (PSC), copper zinc tin sulfide (CZTS) solar cell, quantum dot solar cell (QDSC), organic solar cell (OSC), and dye-sensitized solar cell (DSSC) are the example of the third-generation solar cells. Most of the third-generation solar cells are still in the research stage.

DSSC is a third-generation solar cells co-invented by Michael Gratzel and Brian O'Regan in 1988 at UC Berkeley, USA and further developed by Michael GratzelÉcolePolytechniqueFédérale de Lausanne, Switzerland. The DSSCs are regarded as successful applicants for the substitution of high-cost conventional solar cells. Throughout the last twenty years, Gratzel and hisits colleagues have made considerable efforts to develop further. The different factors involved in the DSSCs system are still under development in several ways to make it ready for commercialization. To date, the maximum 14.7% power conversion efficiency (PCE) has been recorded for the DSSCs [9]. The theoretical PCE limit of the single junction DSSC under standard test conditions (STC) is 32%, according to Professor Michael Graetzel, and a two-level tandem DSSC structure could reach PCE of 46% [10]. Since there is a big difference between theoretical and experimental PCE of DSSC, there is aroom for further improvement. Different researchers have suggested and worked on adifferent methods to improve the PCE of DSSC, such as anode modification by doping material, anode modification by carbon nanotube, surface modification by $TiCl_4$, dye modification, electrolyte modification, and cathode modification by different carbon variant [11–13]. Advancements in DSSCs technology are occurring at an ever-increasing rate, as the development of novel carbon-based materials, such as carbon nanotubes (CNTs). The CNT structure consists of enrolled graphite sheets, in a word, and can be classified as either single-walled (SWCNT) ormulti-walled (MWCNT) depending on its preparation method [14]. Cell performance can be increased by adding SWCNTs/MWCNTs. The incorporation of CNTs into the semiconductor material (i.e., TiO_2, ZnO, SnO_2, ctc.) decreases

the host material's resistance and increases thermal conductivity, electrical conductivity, mechanical strength, and durability. The main aim of using CNTs in the DSSC is to accelerate the flow of electrons from the semiconductor material to the transparent conductive oxide (TCO) glass substrate through the CNTs without any resistance inside the grain boundary [15].

In this book chapter, the next five sections are focused on the basics of DSSCs, CNTs, the effect of CNTs in the cell performance of DSSC, and the degradation study of CNT based DSSC, respectively. In the sixth section, the development of CNT based DSSC is summarized with an outlook. In addition, it is also focused on the improvement of efficiency of DSSC by incorporating carbon nanotubes, which is of great significance for enhancing the performance of DSSC.

2. Dye sensitized solar cell

DSSC is different from other conventional solar cells in terms of both cell architecture and the physical process behind its operation. DSSC combines both solid and liquid phase in contrast to typical crystalline silicon or thin-film solar cell technology based on solid-state semiconductor materials. A typical DSSC consists of a transparent conducting oxide (TCO) glass substrate (i.e., ITO, FTO, AZO, etc.) as an anode, a wide band-gap semiconductor (a nanocrystalline semiconductor material, such as TiO_2, ZnO, SnO_2, $SrTiO_3$, Zn_2SnO_4, and Nb_2O_5, etc. deposited on the TCO), dye sensitizer (anchored on to the surface of nanocrystalline semiconductor material), a volatile electrolyte (I^-/I_3^-, Br^-/Br_3^-, $SCN^-/(SCN)_3^-$, and $SeCN^-/(SeCN)_3^-$, etc. redox couple), and a platinum (or carbon) coated TCO glass substrate as a counter electrode [16–24]. A typical DSSC structure is shown in **Figure 1**.

Figure 2 illustrates the basic operating principle of DSSC. Nanocrystalline semiconductor material (i.e., TiO_2) is deposited on the TCO and provides the indispensable surface area for dye photosensitizer absorption. Photon energy from the sunlight is absorbed (or collected) by the dye photosensitizer layer and produce excited electron (D+) from the highest occupied molecular orbital (HOMO) to the lowest unoccupied molecular orbital (LUMO) (Eq. (1)). The excited dye injects an electron to the conduction band (C.B.) of the semiconductor material and the dye molecule oxidized and losses an electron (Eq. (2)). The injected electron travels
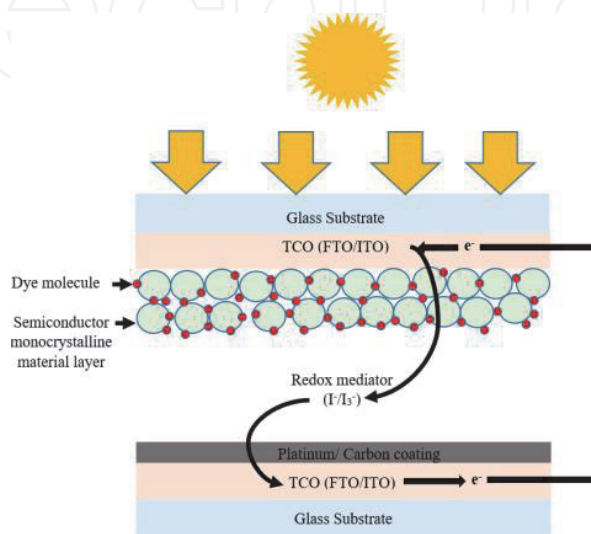

Figure 1.
Basic cell structure of DSSC.

D: Dye sensitizer; D*: Excited dye upon illumination; D+: Oxidized dye
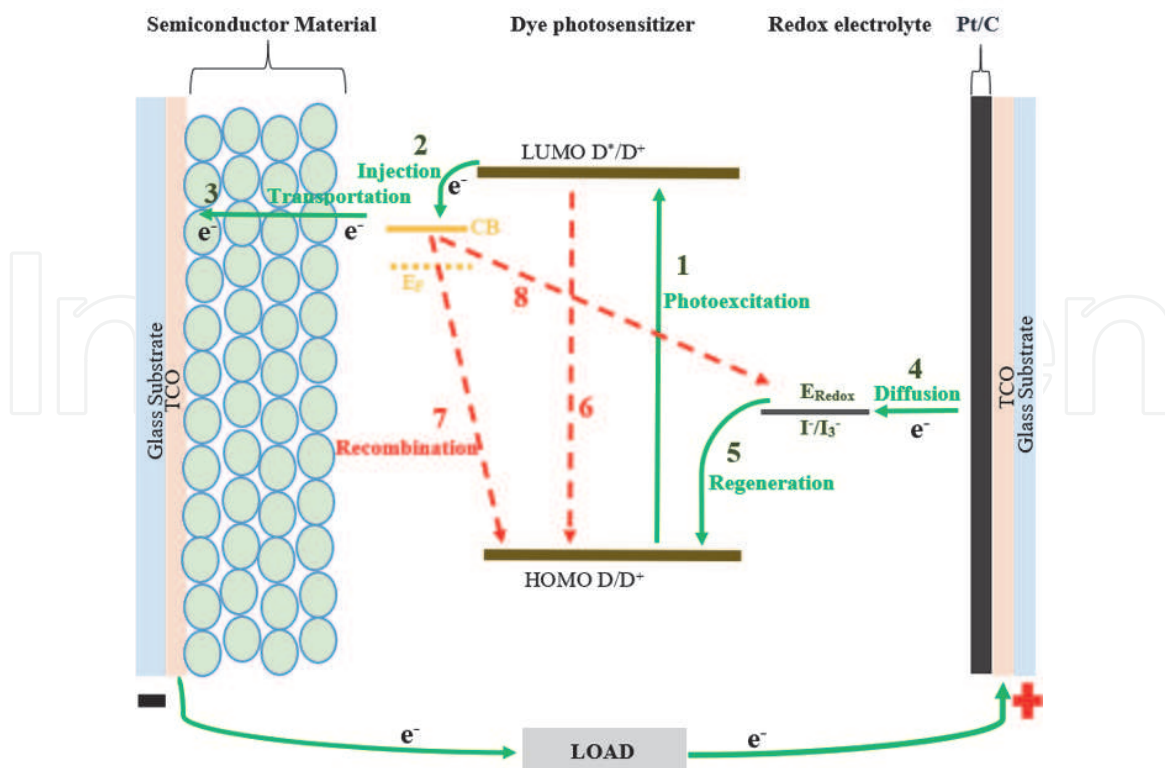

Figure 2.
Basic operating principles of DSSC.

through the semiconductor material toward the anode, and electrical energy is delivered to the external load (Eq. (3)). Then the electron further travels to complete the circuit and reaches the counter electrode (C.E.). The electron is transferred from the C.E. to the electrolyte. Dye regenerates when the dye accepts an electron from the I^- and I^- gets oxidized to I_3^- (Eq. (4)). I_3^- ion float around, and they receive ion from the C.E. (Eq. (5)) [25]. However, some unwanted reaction occurs, such as the recombination of dye (Eq. (6)), dye recombination to the ground state (Eq. (7)), and recombination of electrolyte (Eq. (8)) that reduces the overall cell's electron circulation performance.
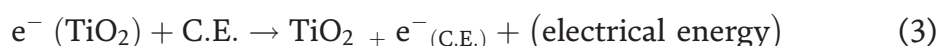
Excitation of dye upon illumination

$$D + h\nu \rightarrow D^* \tag{1}$$

Oxidation of dye due to injection of electrons in TiO_2 photoanode

$$D^* \rightarrow D^+ + e^- (TiO_2) \tag{2}$$

Energy generation

$$e^- (TiO_2) + C.E. \rightarrow TiO_2 + e^-_{(C.E.)} + (\text{electrical energy}) \tag{3}$$

Regeneration of dye

$$D^+ + \frac{3}{2}I^- \rightarrow D + \frac{1}{2}I_3 \tag{4}$$

Restoration of electrolyte at the counter electrode

$$\frac{1}{2}I_3^- + e^-_{(C.E.)} \rightarrow \frac{3}{2}I^- + C.E. \tag{5}$$

Recombination of dye

$$TiO_2|D^* \rightarrow TiO_2|D \tag{6}$$

Dye recombination to ground state

$$TiO_2|D^+ + e^-{}_{(C.B.)} \rightarrow TiO_2|D \tag{7}$$

Recombination of electrolyte

$$I_3^- + 2e^- (TiO_2) \rightarrow 3I^- \tag{8}$$

Green arrows (path (1)–(5)) represent the electron transfer and movement of electrons within the solar cell, while red arrows (path (6)–(8)) represent potential recombination losses within the solar cell.

3. Carbon nanotubes (CNTs)

Carbon nanotubes (CNTs) are hollow cylinders consisting of single or multiple concentric layers of carbon atoms in a honeycomb lattice structure [26]. The CNT structure consists of enrolled graphite sheets, in a word, and can be classified as either or multi-walled (MWCNT) (**Figure 3(a)**) or single-walled CNT (SWNT) (**Figure 3(b)**) depending on its preparation method. In transmission electron microscopy (TEM) studies, MWCNTs were first observed by Iijima in 1991, while SWCNTs were independently developed by Iijima and Bethune in 1993 [26]. CNT has a sp^n hybridization (where n = 2) state of carbon material. However, because of the curved surface of CNT, it does not have a genuine sp^2 hybridization. CNT has a $sp^{2+?}$hybridization, which is in between n = 2 and 3. It is understood that CNT is a material lying between fullerenes and graphite as a new member of carbon allotropes [27]. Carbon nanotubes (CNTs) show very excellent adsorption characteristics because they have a high specific surface area and a nanoscale formation that constitutes many sites. It also has high electrical conductivity, mechanical strength, and a high aspect ratio [28].

3.1 CNT based photoanode in DSSC

CNT incorporated semiconductor material on the conducting electrode surface, offers efficient charge collection and transportation of charge carriers. The electrons
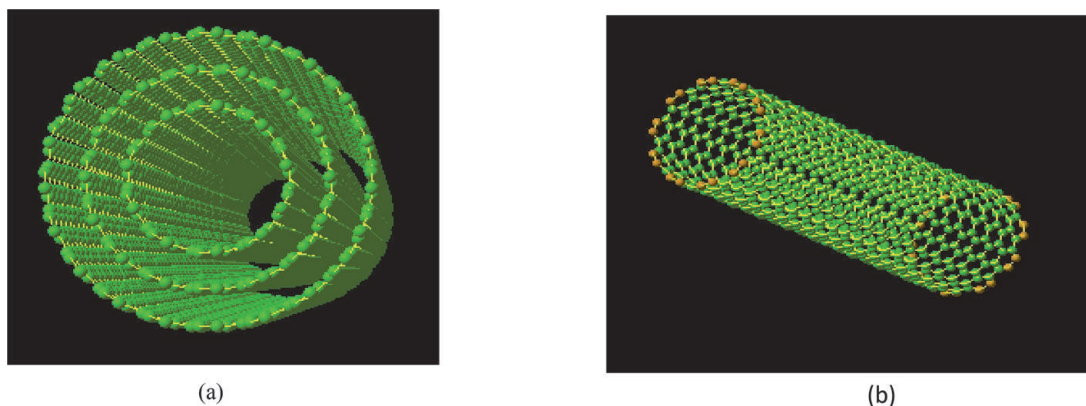

(a)   (b)

Figure 3.
(a) MWCNTs, (b) SWCNTs.

injected from the excited dye into the semiconductor materials are then transferred through a CNT scaffold to generate photocurrent. Such 1-D nanostructures have been successfully exploited to improve the performance of DSSC [29]. **Figure 4** illustrates the role of CNT incorporated semiconductor material (i.e., TiO_2) for efficient electron transportation in DSSC.

Studies by Brown et al. has shown that the presence of CNT (i.e., SWCNT) does not directly affect the primary charge injection process in the D^*/TiO_2 system. SWCNT incorporated TiO_2 ($TiO_2/SWCNT/D^*$) films collect photoinduced electrons more effectively by charge separation than TiO_2/D^* films [29]. Studies have also shown that SWCNT accepts and stores electrons when in contact with photo-irradiated TiO_2 semiconductor materials. The fermi equilibrium with photo-irradiated TiO_2 and SWCNT can store to 1 electron per 32 carbon atoms. When the dyes are linked to the TiO_2-SWCNT suspension, the stored electrons are ready to discharge on demand [30]. SWCNT incorporated TiO_2 showed ~30% higher photoinduced current compared to without SWCNT incorporated TiO_2. Though the SWCNT incorporated TiO_2 based DSSC showed increases in the photoinduced current, the open-circuit voltage degrades in the SWCNT incorporated TiO_2 based DSSC. This phenomenon can be explained by the electron capture properties of SWCNT. At equilibrium condition, a positive shift (~20–30 mV) of the SWCNT causes loweropen-circuit voltage (which is directly related to the difference between fermi level of photoanode and redox electrolyte), as shown in **Figure 5**.

The photoinduced electrons are transferred to the SWCNT network, which minimizes the possibility of charge recombination at grain boundaries [29].

CNTs (i.e., SWCNTs) can be pristine (p-SWCNTs), metallic (m-SWCNTs) and semiconducting (s-SWCNTs) depending on their delocalized electrons occupying a 1-D density of states, chiral angles and diameters. The efficiency of SWCNT/TiO_2 based DSSC depends on different parameters, such as eventual charge separation, charge transfer, charge transport, and recombination rates. Studies by Guai et al. showed that m-SWCNT incorporated TiO_2 based photoanode does not significantly improve the recombination; however, it still enhances cell conversation efficiency of plain TiO_2 based DSSC. This indicates that plain TiO_2 has poor conductivity, which reduces the efficient charge transportation. On the other hand, s-SWCNT incorporated TiO_2 based photoanode showed superior conductivity. s-SWCNT incorporated TiO_2 based photoanode can also suppress the election recombination; thus, significant cell conversion efficiency is observed [31].
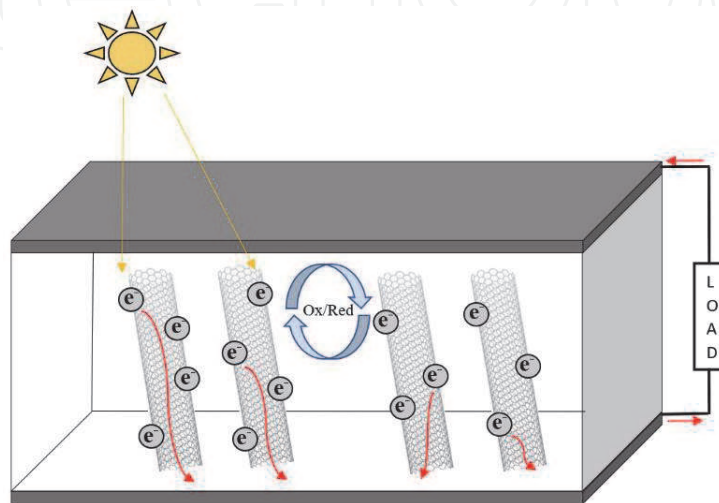

Figure 4.
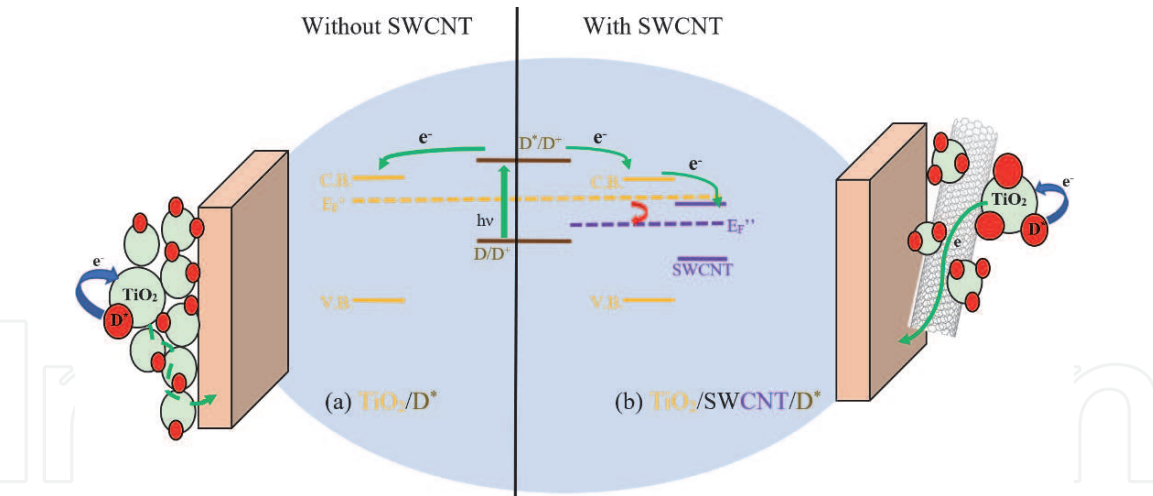*CNT incorporated photoanode for DSSC.*

Figure 5.
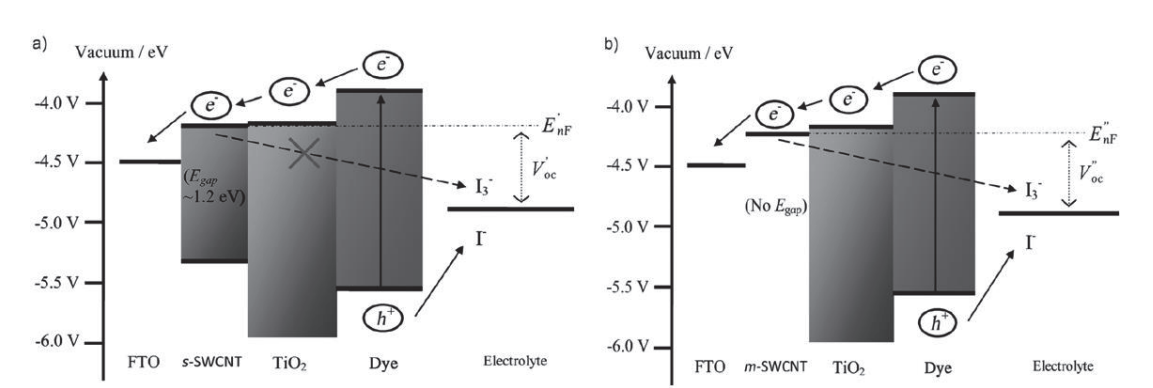*Energy diagram illustrating D*/TiO₂ and transportation of photoinduced electrons without (a) and with (b) SWCNT network.*

Figure 6.
Energy-band diagrams of DSSCs with incorporated (a) s-SWCNTs and (b) m-SWCNTs [31].

Figure 6 illustrates the energy band diagrams of s-SWCNT and m-SWCNT incorporated TiO_2 based DSSC. **Figure 6a** shows the photoinduced electron transfers from the photosensitizer's excited state to the TiO_2 and quickly moves from s-SWCNT to FTO. Since there is less possibility of electrons transported back (or recombination) to the liquid electrolyte to cause I_3^- reduction, more photoinduced electrons are effectively transported and collected by the FTO. This results in enhanced photocurrent generation than p- and m-SWCNT based DSSCs. Also, the effective collections of the photoinduced electron at the anode results in a positive shift in E_{nf}, increasing the open-circuit voltage of the SWCNT/TiO_2 based DSSC. On the contrary, though m-SWCNT has better electron mobility than s-SWCNT, it has a higher disruption in charge carrier transportation, leading to increased back reaction, as shown in **Figure 6b**. As a result, fewer electrons are collected at the FTO, which leads to lower photocurrent and cell conversion efficiency [31]. Hence the relative cell conversion efficiencies can be estimated as follows:

$$TiO_2 > p - SWCNT/TiO_2 > m - SWCNT/TiO_2 > s - SWCNT/TiO_2.$$

However, for the development of the high performance of SWCNT based DSSC, the combination of both m-SWCNT and s-SWCNT is used. Numerous researchers have been working on the combination of m-SWCNT and s-SWCNT. And the w/w % of s-SWCNT varies between 88 and 97% in the mix [32].

The introduction of CNTs into the semiconductor materials causes better dispersion of semiconductor materials particles and smaller crystalline size, structure with high porosity and coarse surface. These results in anincreasein the total surface area thus dye absorption increases and hence overall cell performance. However, the photosensitizer (i.e., metallic photosensitizer, organic photosensitizer, natural photosensitizer) used in DSSCusually anchors on the semiconductor materials (i.e., TiO_2) surface, not the CNT surface. If the mass density of semiconductor materials decreases, the number of dyes loading or absorption will decrease. Thus, if the semiconductor materials are not uniformly distributed on the CNT's surface, total dye absorption will be poor, thereby decreasing the cell's conversion efficiency. To solve this problem, the bonding between semiconductor material and CNTs should be increased. Different research used various methods to solve the problem. CNTs treated with concentrated HNO_3 and H_2SO_4 results in the introduction of -COOH anchoring group on the CNTs, and provides further improved bonding between semiconductor material and CNTs. The acid-treated CNT (i.e., SWCNT) can be used in two ways; either incorporated into the semiconductor material to improve charge transfer or introduced in semiconductor material/electrolyte interface as light scattering centers. In the first case, when acid-treated SWCNTs were incorporated into the semiconductor material (i.e., TiO_2) films, the fabricated DSSC showed a 25% more enhancement in photocurrent than the untreated CNTs. In the second case, when acid-treated SWCNTs were introduced at the TiO_2/electrolyte interface, the value of open-circuit voltage increases, whereas the value of photogenerated current remains constant. The improvement in open-circuit voltagegenerally impliesdecreased dark current and the negative shift of the conduction band of semiconductor material [33, 34]. **Figure 7** illustrates the TiO_2 films with untreated SWCNTs and with acid treated SWCNT.

Similar to SWCNT, MWCNT also improves cell performance. However, the cell performance can be further improved by employing different treatment techniques. Numerous researchers are working on the topics and discovered different methods. Employing these methods can further improve the cell efficiency of DSSC. For example, Zhang et al. introduced RF induced oxygen plasma treatment for the
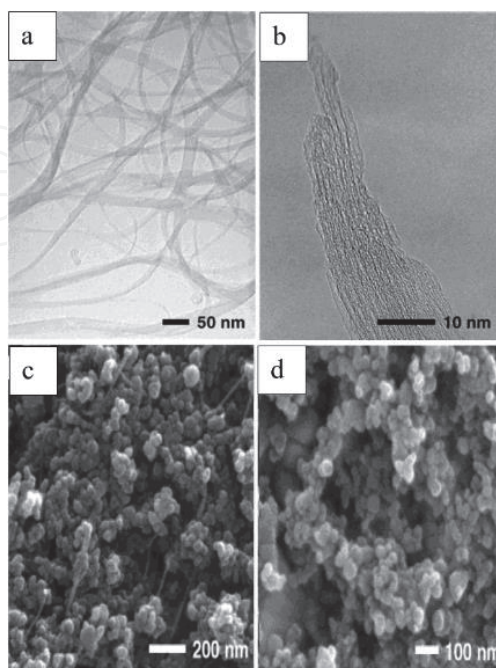

Figure 7.
(a) TEM of untreated bundles of SWCNTs, (b) HRTEM of a single fragmented bundle of acid treaded SWCNTs (c) SEM of TiO₂ films with untreated SWCNTs and (d) SEM of TiO₂ films with acid treated SWCNTs [33].

oxygen containing groups on the surface of the MWCNTs. The oxygen plasma treated MWCNT makes the surface more hydrophilic and improves the dispersion in TiO_2, which leads to high surface area and enhanced dye absorption and hence the cell performance increased. According the Zhang et al. study, the plasma treated MWCNT can improve around 75% cell performance than untreated MWCNT/TiO_2 photoanode based DSSC [34, 35].

Figure 8 illustrates the surface morphology of the coated films of pure TiO_2, MWCNT-TiO_2, and plasma-treated MWCNT-TiO_2 photoanodes using scanning electron microscopic (SEM). The introduction of MWCNT into the TiO_2 semiconductor material causes immobilized uniformly. The FESEM images also indicate thatincorporating MWCNT into the TiO_2 metal oxide material causes a highly porous and coarse surface (**Figure 8b**), which leads to a higher surface area for dye absorption. However, MWCNT-TiO_2 photoanodes has irregular pore sizes and a non-uniform porous structure, which affect the total surface area improvement. On the other hand, plasma treated MWCNT has a higher dispersion in TiO_2 metal oxide material leading to a more uniform porous surface structure (**Figure 8c**), which successfully increases the total surface area for better dye absorption [35].

Researchers have also explored other methods for employing CNTs for high surface area and hierarchical nanoporous structurefor higher cell conversion efficiency. Yun et al. employed TiO_2 hollow sphere/CNT by direct mixing and showed 4.71% with 0.1 wt.% [36]. Muduli et al. sensitized TiO_2/MWCNT composite by hydrothermal method and achieved the crystalline phase, which showed 50% more cell conversion efficiency than the one without the MW-CNTs [37]. Patrick et al. submerged TiO_2 colloid in the optically transparent electrode and electrophoreti-callydeposited SWCNTs for working photoanode. The modified photoanode showed better charge separation and prevented back reaction/recombination, showing 45% improvement in photocurrent [29]. Subha et al. fabricated single-crystalline 1D rutile TiO_2 nanorods/MWCNT composite template-free synthesis method and reported 60% improvement in cell performance. Due to the single
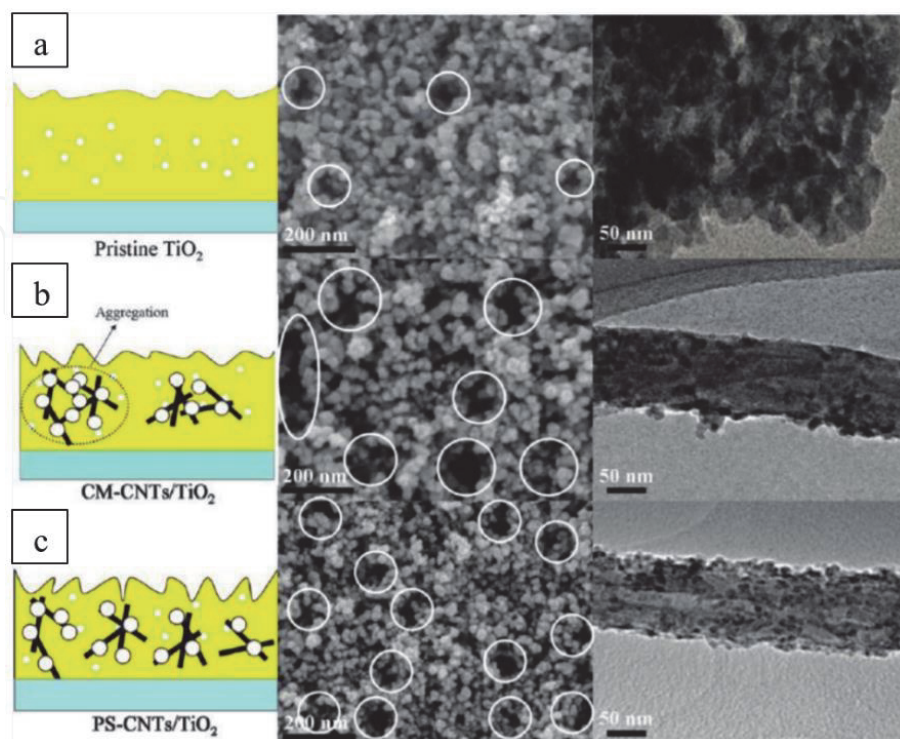

Figure 8.
FESEM and TEM images of the (a) pristine/pure TiO_2, (b) MWCNTs/TiO_2, and (c) plasma treated-MWCNTs/TiO_2photoanode [35].

crystalline structure, there were no grain boundaries, which provides a smooth surface for electron transportation [38]. Zhu et al. sensitized rice grain-shaped TiO_2/MWCNT composite by electrospinning process. Due to the single crystalline structure and high surface area of the rice grain-shaped TiO_2/MWCNT composite, DSSC showed a 32% improvement in cell performance with 0.2 wt.% MWCNT [39].

3.2 CNT based electrolyte in DSSC

In recent years, carbon-based materials in ionic liquids have been investigated as a potential alternative for traditional liquid electrolytes for DSSC application. An effective electrolyte has low viscosity, low vapor pressure, high diffusion coefficient, high electrochemical, and thermal stability. Conventional liquid redox electrolyte has low viscosity and high diffusion coefficient. However, liquid redox electrolyte uses a volatile solvent, which causes a problem in the commercialization of DSSC, such as cell leakage of electrolyte, performance degradation, high-temperature instability, and pressure build-up after in the fabricated cell due to the volatile solvent. Also, liquid electrolyte creates obstacles for the flexible structure and large-scale solar cell. Quasi-solid-state electrolytes based on ionic liquids can easily solve the drawbacks of liquid electrolyte efficiently. Organic hole conducting materials, p-type inorganic semiconductors, or different nano-components (i.e., graphene, CNTs) were diffused into ionic liquids to the sensitized quasi-solid-state electrolyte for DSSC application. **Figure 9** shows a basic schematic diagram of a CNT based electrolyte for DSSC.

3.3 CNT based cathode in DSSC

In recent years, carbon-based materials, such as graphite, carbon black, and carbon nanotubes, have been studied to replace traditional platinum (Pt) counter
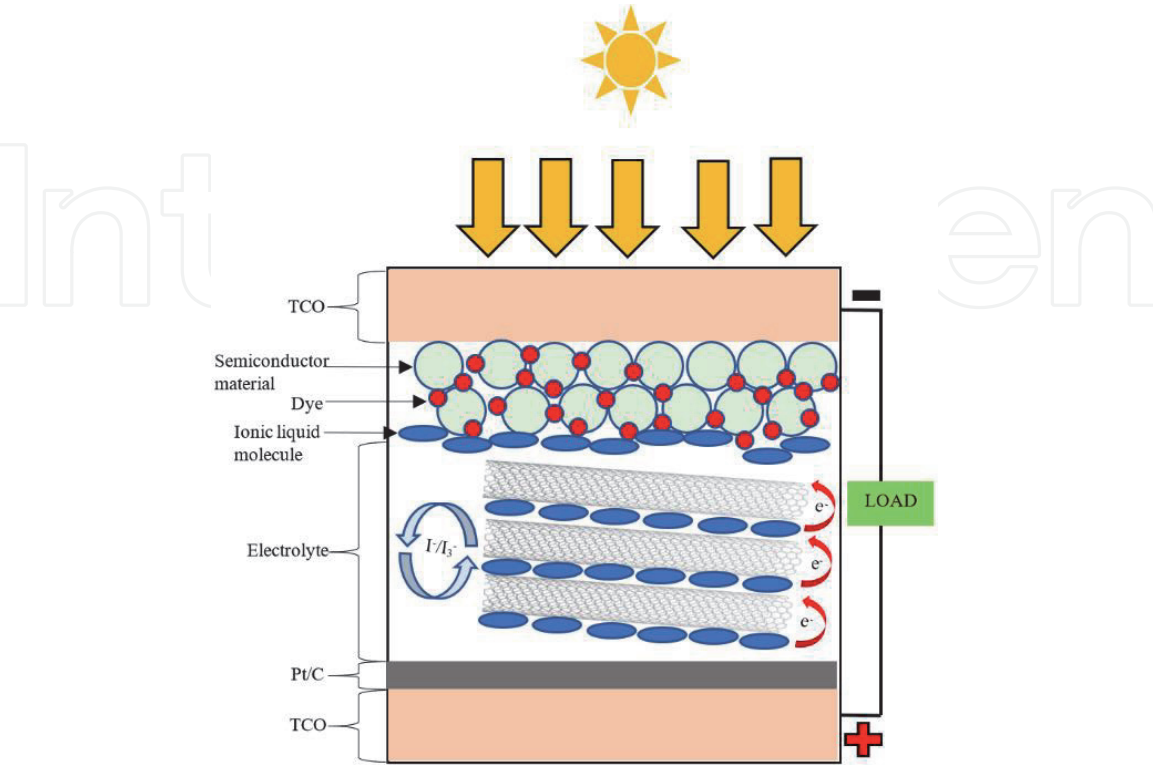

Figure 9.
CNT based electrolyte for DSSC application.

electrodes for low-cost DSSC. Carbon materials are not only abundant but also highly resistant to corrosion. Carbon-based material, especially CNT, has attracted considerable interest because of its fast electron transfer kinetics and large surface area. **Figure 10** shows a basic schematic of a CNT based counter electrode for DSSC.

Different methods have been explored for CNT based counter electrode. Nam et al. used paste printing and CVD growing methods for the counter electrode. The paste printing MWCNT based counter electrode based DSSC has lower cell efficiency (8.03%) than the Pt. counter electrode based DSSC's cell efficiency (8.80%). However, the CVD has grown MWCNT had higher cell conversion efficiency (10.04%) than the Pt. counter electrode based DSSC's cell efficiency (8.80%) [40]. Ramasamy et al. fabricated spray-coated MWCNT counter electrode and showed the effect of spray time/coating thickness [41]. Widodo also fabricated spray-coated CNT on FTO glass substrate for counter electrode for DSSC [42]. Prasetio et al. used different weight (0.01, 0.02 and 0.04 gram) of CNT and observed the cell performance of DSSC [43]. **Figure 11** illustrates the SEM of (a) the surface and (b) the cross-section CNT based counter electrode [43].

4. Effect of CNT on the cell performance of DSSC

4.1 Effect of CNT based photoanode on the cell performance of DSSC

As mentioned earlier (in Section 3.1.), adding CNT nanoparticles into mesoporous structure provides a strong light-harvesting capability and a large surface area for high-efficiency DSSC. Mesoporous semiconductor materials anchor on the long tubular CNT's outer surface and this assembly ensure efficient electron transport through CNTs. CNT improves the electron transport and increases the coating's thickness; thus, dye building on the anode material increase. CNT results in gains in the photocurrent without compromising the electron injection to the electrode.

From the previous discussion (Section 3.1.), CNT can be used either CNT/semiconductor material composite photoanode or counter electrode. For CNT-based photoanode for different types of dyes, such as metal complex dye sensitizer, natural dye sensitizer has been explored for DSSC operation.
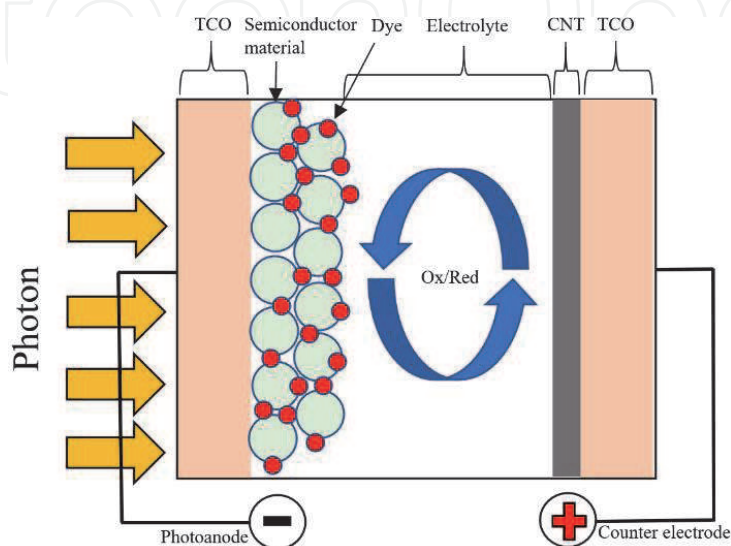

Figure 10.
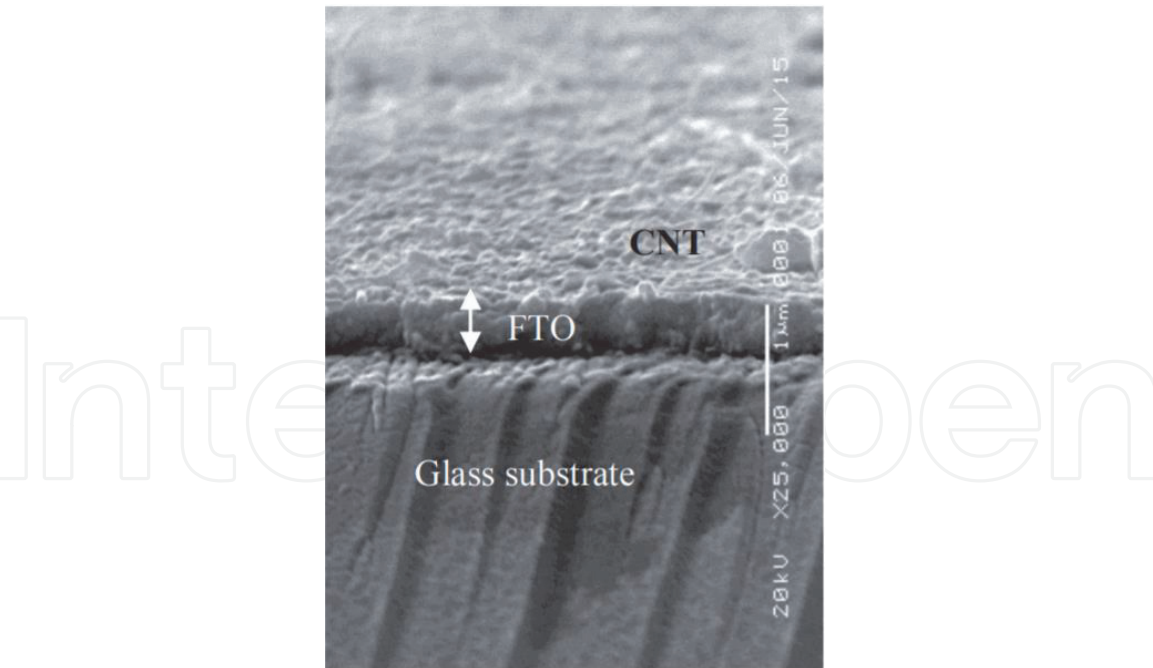*CNT based counter electrode for DSSC.*

Figure 11.
SEM of the cross-section CNT based counter electrode [43].

Photoanode	J_{sc} (mA/cm^{-2})	V_{oc} (V)	Fill factor (FF)	Efficiency (%η)	Improvement (%)
PristineTiO$_2$	6.48	0.84	0.65	3.63	
Chemically modified CNT/TiO$_2$	8.56	0.83	0.66	4.66	28
O$_2$ plasma treated CNT/TiO$_2$	11.04	0.85	0.68	6.34	75

Table 1.
Different CNT/TiO$_2$ photoanode based DSSC [35].

Zhang et al. used N719 dye on the CNT photoanode-based DSSC. They prepared two different types of CNT based photoanode: pristine, chemically modified, and O$_2$ plasma-treated CNT. For chemically modified CNT, 500 mg CNT was mixed with 100 ml H$_2$SO$_4$/HNO$_3$ solution (1:1) and kept at 140°C for 6 hours. Afterward, the solution was filtered, cleaned with distilled water, and vacuum dried. For O$_2$ plasma-treated CNT, CNT was treated with O$_2$ plasma treated for 40 minutes at 0.26 Torr (at 50 W) [35].

O$_2$ plasma-treated CNTs/TiO$_2$ photoanode based DSSCs has more uniform holes and rough surface, which provides higher dye adsorption and less charge recombination than either TiO$_2$ or chemical modified CNTs/TiO$_2$. The O$_2$ plasma-treated CNTs/TiO$_2$ photoanodebased DSSC showed 6.34% cell efficiency, which is ~75% higher than the conventional TiO$_2$ photoanode based devices (**Table 1**). **Figure 12** illustrates the I-V characteristics of pristine TiO$_2$, chemically modified CNT/ TiO$_2$, and O$_2$ plasma-treated CNT/ TiO$_2$ photoanode based DSSC with N719 dye. The value of the open-circuit voltage of chemically modified CNT/ TiO$_2$ based DSSC was lower than the TiO$_2$ photoanode based DSSC because of poor adhesion between chemically modified CNT/TiO$_2$; however, the overall cell conversion efficiency was 28% higher than the traditional TiO$_2$ based DSSC [35].

Dembele et al. sensitized an ethanolic suspension of MWCNTs (0.006 g of MWCNTs in 15 mL of ethanol) and then mixed with a known weight of TiO$_2$ paste
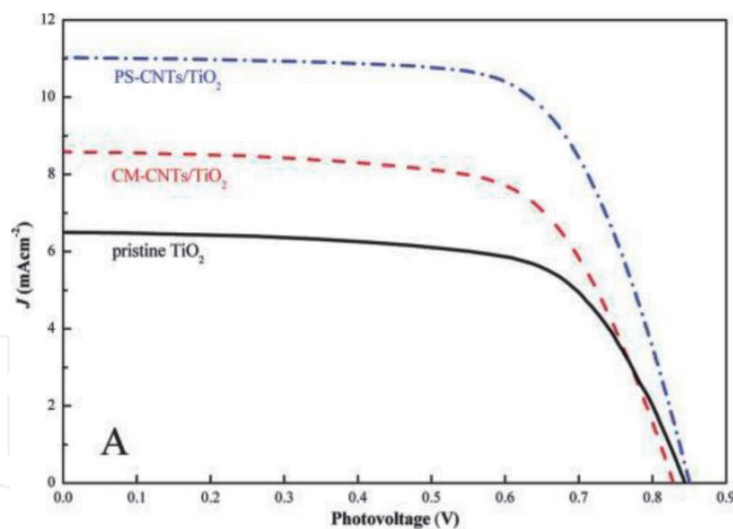
Figure 12.
I-V characteristics of pristine TiO₂, chemically modified CNT/ TiO₂ and O2 plasma treated CNT/TiO₂
photoanode based DSSC with N719 dye [35].

to obtain a fixed percentage of MWCNT/TiO$_2$ composite. The MWCNT/TiO$_2$ composites were tape cast on FTO glass substrate. The concentration of MWCNTs was varied in the range of 0–0.250 wt. %. The fabricated photoanodes were soaked in a 0.5 mM ethanolic solution of N719 sensitizer. They were increasing the percentages of MWCNTs in the MWCNT/TiO$_2$ composite, which results in a slight improvement in dye loading (from 0.010–0.020%). In comparison, the average number of dye mole per volume unit improved almost 3.5 times for the 0.25 wt.% MWCNT/TiO$_2$film than the pure TiO$_2$film. However, this chemisorption of dye multilayers are detrimental for overall cell efficiency: for optimum cell efficiency, the dye should be chemisorbed in a closely packed monolayer. **Figure 13** illustrates the SEM image of the bare TiO$_2$ and MWCNT (0.25 wt.%)/TiO$_2$ film [44].

From **Table 2**, optimized concentration (0.010–0.020 wt.%) of MWCNTs based TiO$_2$ photoanode significantly increases the overall cell conversion efficiency. Introducing a reflection layer into the cell increases the electron lifetime and decreases recombination, leading to improved overall cell performance and photoconversion efficiency (9.0%) [44].

Not only DSSC sensitized with metallic dye, but also DSSC sensitized with natural dye shows similar characteristics to the concentration of CNT (i.e., MWCNT). Kabir et al. used natural yellow dye sensitizer extracted from the turmeric (*Curcuma longa*). They have fabricated DSSC with natural yellow dye as a sensitizing source for TiO$_2$ photoanode with different MWCNT concentrations. The concentration of MWCNT ranges from 0.005 wt. % to 0.050 wt. %. **Figure 14** shows surface morphology of (a) bare TiO$_2$, (b) MWCNTs, (c) MWCNTs/TiO$_2$, and (d) TiCl4 treated MWCNTs/TiO$_2$ film [45].

The integration of MWCNTs improved the cell efficiency of the DSSC by developing a special charge carrier transport channel that is distributed uniformly throughout the TiO$_2$ semiconductor. Cell efficiency of all concentrations of MWCNT incorporated by TiO$_2$ is higher than that of the without MWCNT incorporated by TiO$_2$. The concentration of the MWCNT from 0.000 wt. % to 0.015 wt. %, cell efficiency has improved dramatically (From **Table 3**). The optimum concentration is 0.015 wt. % MWCNTs have a maximum cell efficiency of 1.653%, whereas for without MWCNT integrated TiO$_2$, cell efficiency is 0.921%. After achieving the best possible combination, further increasing the concentration of MWCNT leads to a negative effect on cell parameters such as I$_{sc}$, V$_{oc}$, and FF.
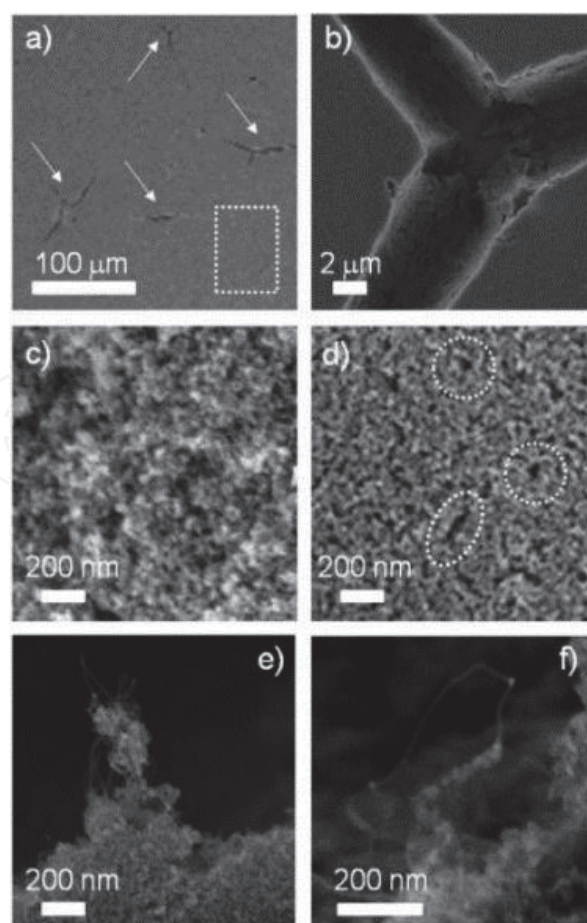
Figure 13.
SEM images of (a, b, d, e, f) the 0.25 wt.% CNT photoanode at various magnifications, and (c) bare TiO$_2$ photoanode [44].

Higher concentrations of MWCNTs result in a loss of transparency and low absorption of light, which decreases the photogenerated current [45].

4.2 Effect of CNT based electrolyte on the cell performance of DSSC

As mention earlier (Section 3.2.), CNT based electrolyte not only enhance cell performance of DSSC but also provide improvement in cell structure. Ahmad et al. sensitized a new type of quasi-solid-state electrolyte by dispersing graphene and CNT into the 1-methyl 3-propyl imidazolium iodide (PMII) ionic liquid. They also varied the CNT (i.e., SWCNT) content from 1 wt.% to 16 wt.% in the PMII ionic liquid. Maximum cell efficiency of 1.43% was observed for 7% SWCNT +93% PMII ionic liquid electrolyte (**Table 4**). They have also combined graphene with SWCNT and observed the effect of SWCNT in the quasi-solid-state electrolyte in DSSC application. Combining SWCNT and graphene with PMII enhances cell performance significantly, which is higher than both SWCNT + PMII combination and PMII (**Table 5**) [46].

Lee et al. sensitized MWCNT–polymethyl methacrylate (PMMA) composite electrolyte by thermal polymerization for solid state DSSC. The MWCNT-PMMA composite has made a homogenous solution of 0.26 g MWCNT, 5 g of methyl methacrylate (MMA), and 2-hydroxy-2-methyl-propylphenone (initiator). The solution was vacuum dried and cleaned thoroughly (with dichloroethane (DCE) to remove initiator residue). The MWCNT-PMMA composite was mixed with iodide couples (0.1 M of LiI, 0.015 M of I2, and 0.2 M of t-butyl pyridine) in acetonitrile solvent and stirred for 20 hours for MWCNT-PMMA composite electrolyte.

Anode structure	CNTs (wt %)	$T_{annealing}$ (°C)	Thickness (μm)	PCE (%)	FF (%)	V_{oc} (mV)	J_{sc} (mA cm^{-2})	Dye loading (mol mm$^{-3} \times 10^7$)
Transparent layer	0	450	12.6	6.5	71.0	745	12.7	1.05
Transparent layer	0.003	450	12.5	5.6	68.0	700	11.9	
Transparent layer	0.007	450	11.5	6.4	67.1	695	13.8	
Transparent layer	0.010	450	12.8	8.1	71.0	724	15.6	1.05
Transparent layer	0.015	450	9.9	7.9	71.0	734	15.3	1.65
Transparent layer	0.020	450	11.3	7.4	71.0	704	14.8	1.25
Transparent layer	0.045	450	8.8	6.7	71.0	698	13.6	1.35
Transparent layer	0.075	450	10.1	5.9	73.0	707	11.6	1.35
Transparent layer	0.250	450	16.4	1.1	62.0	789	2.2	3.70
Transparent layer + reflecting layers	0	500	15.9	7.0	69.0	755	13.6	
Transparent layer + reflecting layers	0.010	500	16.4	9.0	74.0	758	16.0	

Table 2.
Effect of CNT (MWCNT) concentration in the cell performance of N719 bye based DSSC [44].

Figure 15 shows the FESEM image of MWCNT and MWCNT-PMMA composite, and **Figure 16** illustrates the TEM and HR-TEM images MWCNT and MWCNT-PMMA composite [47].

Table 6 lists the photovoltaic performance of DSSC fabricated with MWCNT-PMMA composite. Lee et al. Lee et al. achieved higher cell efficiency of 2.9% (than the reference cell's efficiency of 1.9%), which was possible because of enhanced amorphous structure and ionic conductivity [47].

4.3 Effect of CNT based counter electrode on the cell performance of DSSC

To achieve high cell performance in a large application area, platinum is used for its excellent electrochemical activity. However, using Pt as a counter electrode increases overall cell cost. Many efforts have been made for large surface area and fast electron transportation to apply CNTs to the cathode. CNTs prices are lower than Pt, but it has high electrochemical activity, which makes DSSCs commercially viable. Prasetio et al. sensitized CNT-based cathode by doctor blade method and observed CNT concentration's effect by varying the weight of CNT (0.01, 0.02, and 0.04 g). A slurry was prepared by mixing a fixed mass of (0.01 or 0.02 or 0.04 g) CNT, 0.2 g ethylcellulose, 2 ml ethanol, and 0.8 g terpineol. The slurry was doctor bladed on FTO substrate and dried in the air, followed by annealing at 450°C for 60 minutes. **Figure 17** illustrates SEM images of prepared CNT cathode fabricated with different CNT masses (0.01, 0.02, and 0.04 g) [43].[Use the similar format for gram, either g or gr or gram throughout the chapter].

Table 7 lists the photovoltaic performance of DSSC fabricated with different masses of CNT as a cathode. Increasing the mass of CNT in the cathode increases the photogenerated current; however, CNT does not increase other cell parameters, such as open-circuit voltage and fill factor. An increase in short circuit current resulted in higher cell conversion efficiency.

Ramasamy et al. spray-coated MWCNT on FTO and used it as a cathode. Dispersed MWCNT was sprayed onto FTO glass substrate with a spray gun, which was
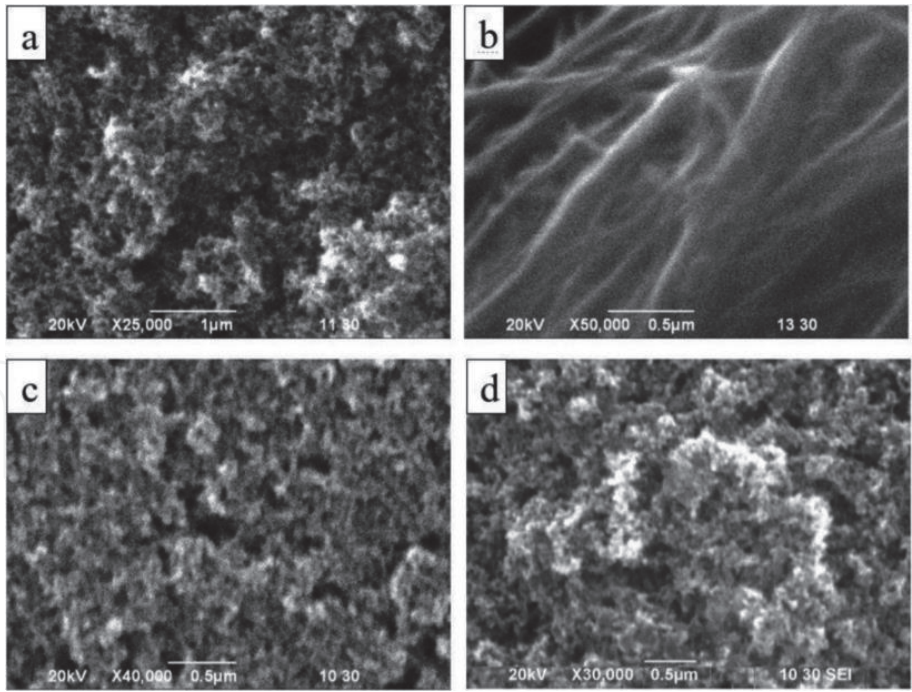
Figure 14.
SEM image of (a) bare TiO₂, (b) MWCNTs, (c) MWCNTs/TiO₂, and (d) TiCl₄ treated MWCNTs/TiO₂ film [45].

MWCNT concentration	V_{OC} (V)	I_{sc} (mA)	FF	η%	Dye loading (mol mm^{-3} × 10^7)
0 wt.%	0.515 ± 0.010	3.792 ± 0.024	0.472 ± 0.007	0.921 ± 0.037	1.13
0.005 wt.%	0.512 ± 0.008	4.973 ± 0.017	0.535 ± 0.003	1.362 ± 0.038	1.15
0.010 wt.%	0.513 ± 0.001	5.346 ± 0.011	0.564 ± 0.001	1.546 ± 0.008	1.22
0.015 wt.%	0.502 ± 0.006	5.995 ± 0.028	0.553 ± 0.009	1.653 ± 0.054	1.37
0.020 wt.%	0.499 ± 0.005	5.119 ± 0.023	0.549 ± 0.010	1.404 ± 0.046	1.34
0.025 wt.%	0.498 ± 0.001	4.873 ± 0.020	0.522 ± 0.002	1.267 ± 0.017	1.31
0.030 wt.%	0.489 ± 0.004	4.543 ± 0.018	0.504 ± 0.006	1.119 ± 0.027	1.28
0.040 wt.%	0.486 ± 0.011	4.543 ± 0.023	0.499 ± 0.008	1.080 ± 0.047	1.28
0.050 wt.%	0.481 ± 0.013	4.361 ± 0.028	0.494 ± 0.003	1.036 ± 0.041	1.25

Table 3.
I-V performance of different concentrations of the MWCNT incorporated TiO₂ based DSSC fabricated with natural yellow dye [45].

SWCNT content (wt%)	J_{sc} (mA/cm^2)	V_{oc} (V)	FF	Efficiency (%)
0% (only PMII)	0.370	0.575	0.64	0.16 ± 0.01
1%	0.524	0.573	0.70	0.25 ± 0.01
7%	5.19	0.540	0.41	1.43 ± 0.13
10%	2.15	0.616	0.36	0.56 ± 0.02
13%	1.64	0.614	0.41	0.46 ± 0.02
16%	2.09	0.541	0.32	0.40 ± 0.02

Table 4.
I-V performance of DSSCs with quasi-solid-state electrolytes containing different wt.% of SWCNTs in PMII [46].

Content (wt%)	J_{sc} (mA/cm^2)	V_{oc} (V)	FF	Efficiency (%)
100% PMII	0.370	0.575	0.64	0.16 ± 0.01
85% PMII +3% SWCNT +12% graphene	7.32	0.594	0.44	2.50 ± 0.10
85% PMII +12% SWCNT +3% graphene	4.66	0.561	0.43	1.39 ± 0.10

Table 5.
I-V performance of DSSCs with quasi-solid-state electrolytes containing different wt.% of SWCNT and graphene in PMII [46].
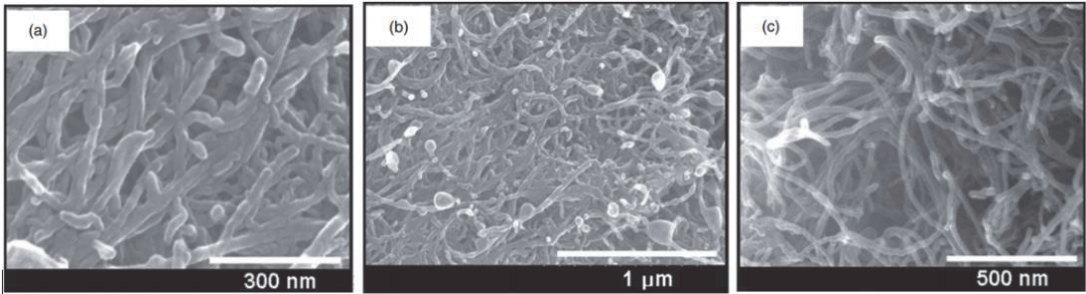

Figure 15.
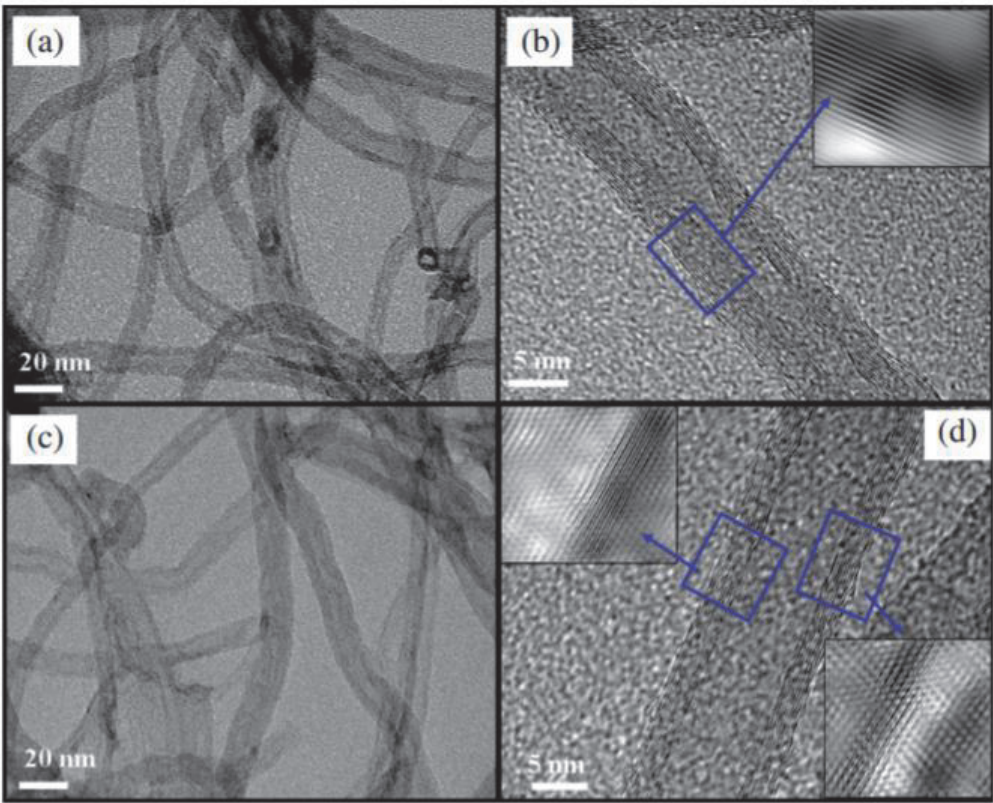*SEM images of (a) MWCNT, and (b and c) MWCNT–PMMA composite film [47].*

Figure 16.
TEM and HR-TEM images of (a, c) MWCNT and (b, d) MWCNT–PMMA composites [47].

connected to an air compressor. Ramasamy et al. varied the spray time and observed the effect of spraying time on the cell performance of DSSC. Since the spray time is directly related to the thickness of the MWCNT layer, in other words, they have observed the effect of MWCNT coating thickness on the cell performance of DSSC [41].

Sample	Differential scanning calorimetry (DSC) data		Conductivity (mS/cm)	Photovoltaic performance			
	Melting temperature T_m (°C)	Heat of melting ΔH (J/g)		J_{sc} (mA/cm^2)	V_{oc} (V)	FF (%)	Efficiency (%)
PEO	74.3	119..5	1.2	5.7	0.61	53.4	1.9
MWCNT-PMMA	81.2	97.8	2.3	8.9	0.57	61.8	2.9

Table 6.
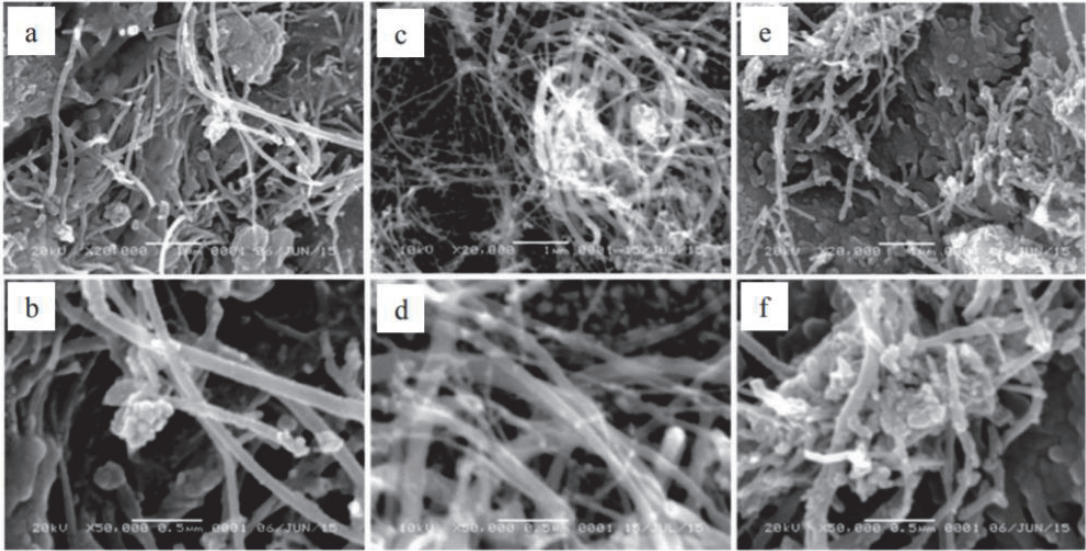*I-V performance of DSSC fabricated with MWCNT-PMMA composite [47].*

Figure 17.
SEM images of prepared CNT cathode fabricated with different masses of the CNT (a, b) 0.01 gram (c, d) 0.02 gram, and (e, f) 0.04 gram [43].

Mass of CNT in cathode (in gram)	J_{sc} (mA/cm^2)	V_{oc} (V)	FF (%)	Efficiency (%)
0.01	2.093	0.49	31	0.32
0.02	4.829	0.48	32	0.74
0.04	6.413	0.45	32	0.91

Table 7.
I-V performance of DSSC fabricated with different mass of CNT as cathode [43].

Table 8 lists the I-V parameters of various spraying times of the MWCNT counter electrode. The value of open-circuit voltage is more or less independent of the spray time; however, both short circuit current and fill factor showed a strong dependence on the spraying time of MWCNTs. The charge transfer resistance of the MWCNT cathode in the iodide/tri-iodide electrolyte solution was decreased by increasing the spraying time, which results in a significant improvement in the cell performance of the MWCNT counter electrode based DSSC [41].

Nam et al. used two different methods for CNT counter electrode-based DSSC: screen printing and chemical vapor deposition. Screen printed MWCNT cathode based DSSC showed lower cell performance (8.03%) than the reference Pt cathode based DSSC's cell performance (8.80%) because of unfavorable contact resistance between the MWCNT and FTO. On the contrary, chemical vapor deposited

Spraying time (s)	V_{oc} (V)	J_{sc} (mA/cm^2)	FF (%)	Efficiency (%)
Bare FTO	0.428	1.48	0.07	0.04
5	0.772	8.03	0.11	0.68
10	0.784	12.81	0.15	1.51
30	0.773	15.67	0.28	3.39
60	0.778	15.92	0.47	5.82
100	0.778	15.86	0.57	7.03
200	0.783	15.64	0.62	7.59

Table 8.
I-V performance of DSSC fabricated with MWCNT based cathode [41].

Cathode	J_{sc} (mA/cm^2)	V_{oc} (V)	FF (%)	Efficiency (%)
Reference Pt coated cathode	17.68	746.27	0.65	8.80
Paste printed MWCNT cathode	15.27	738.43	0.69	8.03
CVD grown MWCNT cathode	17.62	755.89	0.73	10.04

Table 9.
I-V performance of DSSC with different MWCNT based cathode (different deposition method for MWCNT) [40].

$H_2PtCl_6.6H_2O$ (%)	SWCNT (%)	Light transmittance (%)	J_{sc} (mA/cm^2)	V_{oc} (V)	FF (%)	Efficiency (%)
0.24	0	87	7.29	0.74	0.56	3.00
0.48	0	83	9.42	0.74	0.68	4.71
0.72	0	72	5.86	0.75	0.67	2.91
0.48	0.03	81	9.61	0.75	0.68	4.88
0.48	0.06	80	11.20	0.75	0.71	5.96
0.48	0.012	74	8.53	0.75	0.68	4.33

Table 10.
I-V performance of DSSC fabricated with different $H_2PtCl_6.6H_2O$ and SWCNT content [48].

MWCNT cathode based DSSC showed higher cell performance (10.04%) due to aligned MWCNT and improved charge carrier conduction path (**Table 9**) [40].

Xiao et al. used Pt/SWCNT film to spray onto the ITO coated polyethylene naphthalate substrate using a vacuum thermal decomposition method at 120°C. The fabricated cathode showed higher light transmittance, higher chemical stability, higher electrocatalytic activity for redox electrolyte, and lower charge carrier transfer resistance [48]. **Table 10** lists the photovoltaic properties of DSSC fabricated with different $H_2PtCl_6.6H_2O$ and SWCNT content [48].

5. Prospects of CNT in DSSC application

DSSCs have attracted considerable attention due to their simple fabrication process, inexpensive raw materials, and employment of eco-friendly materials. Recently, to take advantage of their lower electrical resistance, excellent electrocatalytic operation, mechanical integrity, low cost, and flexibility, CNTs

have been incorporated into DSSCs. Kongkaland et al. used a different approach using carbon fiber electrodes (CFE) than conventional transparent conduction oxide, such as ITO, FTO, etc. They have deposited TiO_2 semiconductor material on the CFE and CFE-SWCNT film. The incorporation of SWCNT in the CFE increased cell performance from 7.36–16%. This two times improvement in the cell
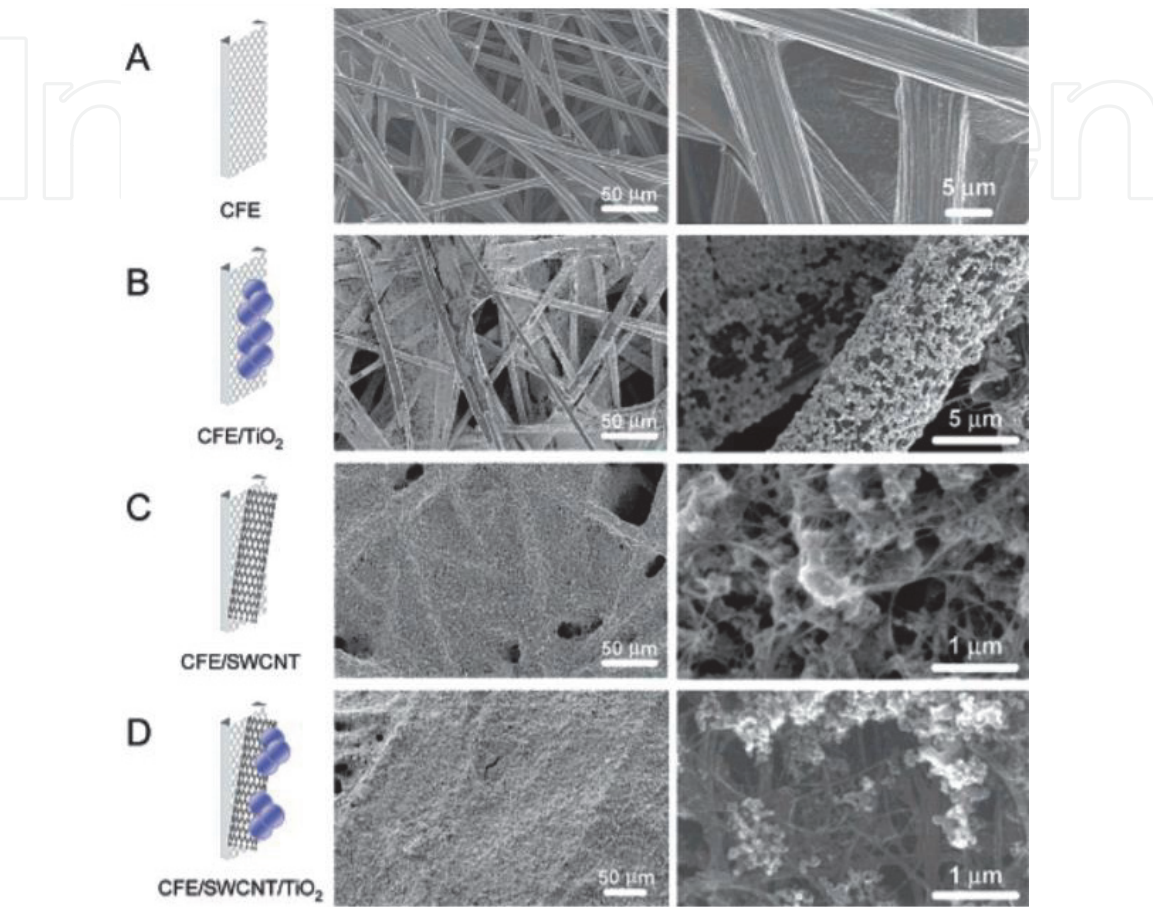

Figure 18.
SEM of a (A) CFE before surface modification; (B) deposition of TiO_2 on CFE film; (C) electrophoretic deposition of SWCNT on CFE; (D) after deposition of deposition of TiO_2 on CFE-SWCNT film [49].
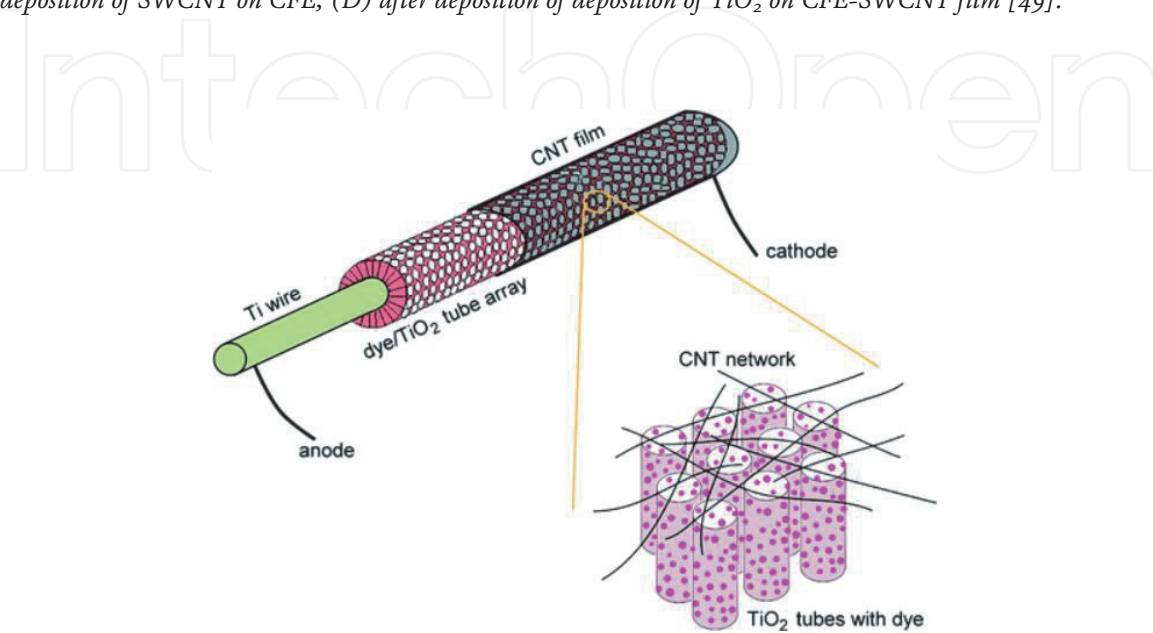

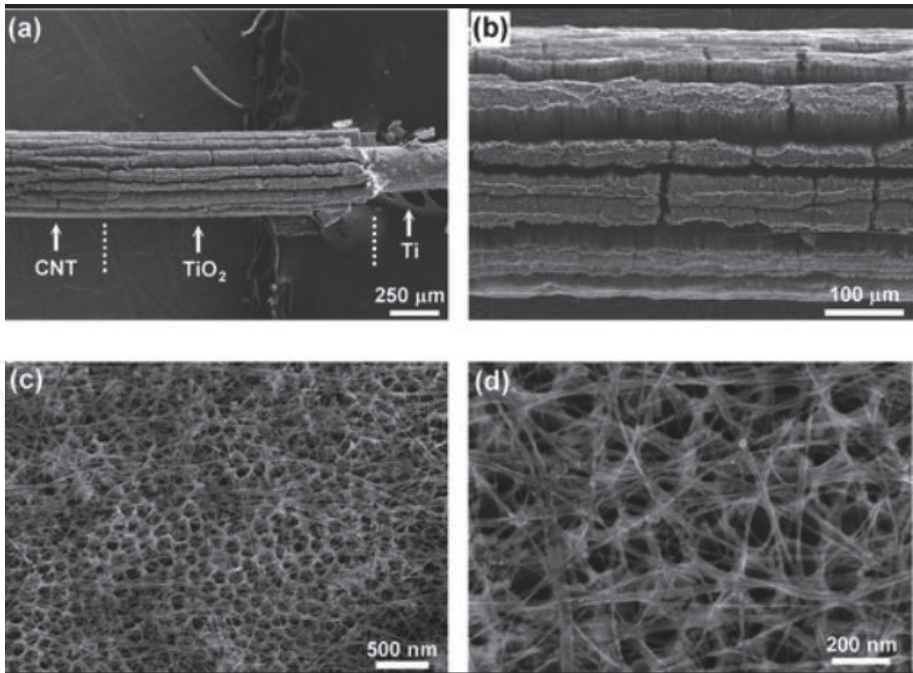**Figure 19.**
Coaxial single-wire structure DSSC [50].

Figure 20.
SEM image of (a) different parts of the wire, (b) a wire section uniformly wrapped by CNT film. (c) CNT network deposited on porous TiO$_2$, and (d) CNT-TiO$_2$ nanotubes [50].
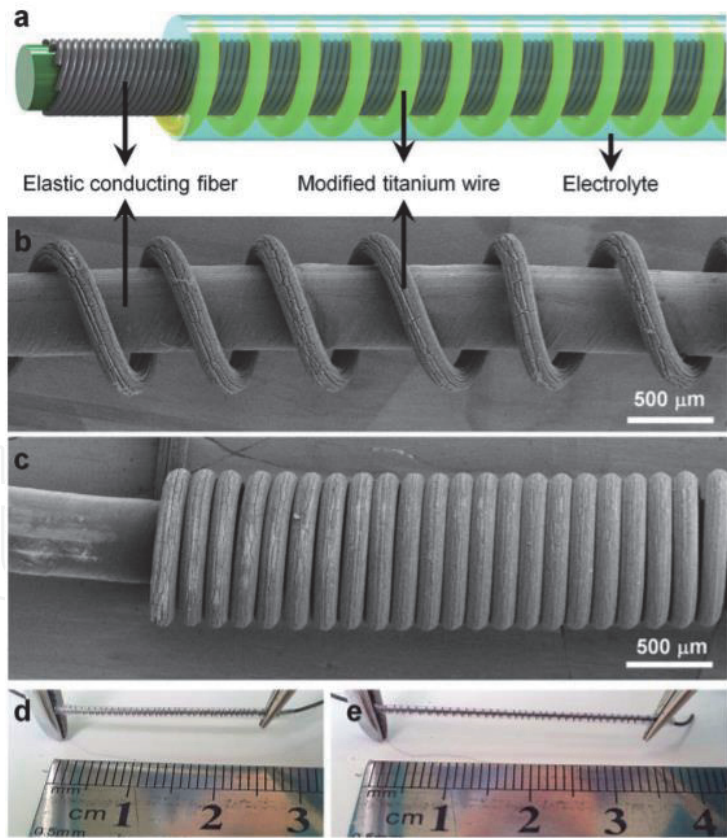

Figure 21.
(a) Basic structure of a textile DSC (b) SEM images of a textile DSC with 560μmpitch distances (c) SEM images of a textile DSC with 164 μm pitch distances, (d) A textile DSC before and after stretch by 30%, and (e) A textile DSC after 30%stretch [51].

performance indicates that CNTs can serve a valuable role in facilitating charge collection in DSSC application. **Figure 18** illustrates the SEM image of CFE and CFE-SWCNT base anode for DSSC application [49].

Powering next-generation wearable/implantable biomedical devices, or smart textile, have gained extensive attention in recent years. Among the developed energy harvesting devices, DSSCs cell structures have become ideal candidates for developing practical self-powered biomedical devices or smart textile due to their lightweight, flexibility, high power-per-weight ratios, and superior mechanical stability/robustness. The conventional planar-shaped DSSCs with sandwich-like configuration includes five primary parts: TCO, an anode (semiconductor material), dye, redox electrolyte, and cathode (Pt/C). Based on the conventional planar structure, DSSCs can also be made into flexible configurations. Zhang et al. fabricated fiber-shaped DSSC and made a double-wire structure (shown in **Figure 19**). They have manufactured a flexible DSSC structure on a single wire (Ti-TiO$_2$) and wrap the CNT around the tube array. CNT provides full contact with the active layer, unlike Pt, and provides uniform light absorption throughout the entire circumference ofDSSC [50]. **Figure 20** illustrates the fabricated fiber shaped DSSC [50].

Yang et al. further developed a wearable DSSC textiles method based on electrically conducting fibers. They have prepared fiber electrodes by aligning winding multiwalled carbon nanotube (MWCNT) sheets on rubber fibers. The working fiber electrode was prepared by incorporating modified Ti onto the MWCNT fiber electrode (**Figure 21c**). The wire-shaped DSSCs could weave into wearable photovoltaic textile solar cells. The maximum cell efficiency of the wire-shaped DSSC reached 7.13% [51].

6. Conclusion

Incorporating CNT in the DSSC increases the interaction between electrodes and electrolyte, enhancing the cell performance of DSSC. In addition, incorporating CNT in the semiconductor material decreases resistance to the grain boundaries. It provides a unique charge carrier transport channel distributed uniformly in the host semiconductor to absorb the charge carrier from the collector. Cell performance of CNT based photoanode can be improved by optimizing the CNT concentration and deposition method. For CNT based electrolyte, the ionic electrolyte can be an alternative for traditional redox electrolyte. Also, CNT based ionic electrolyte provides better cell performance with enhanced durability. Finally, the CNT-based cathode can offer a large surface area and fast electron transportation, which reduces the chances of recombination.

Lastly, incorporation of CNTs into DSSC will serve a significant role in producing solar cells that produce energy at an affordable rate relative to the existing energy generation approaches. New methods are frequently being published and will present opportunities for innovation in both research and industrial growth.

Author details

Md. Mosharraf Hossain Bhuiyan[1,4*†], Fahmid Kabir[2†], Md. Serajum Manir[3],
Md. Saifur Rahaman[1], Prosenjit Barua[2], Bikrom Ghosh[2], Fumiaki Mitsugi[5]
and Tomoaki Ikegami[5]

1 Institute of Nuclear Science and Technology, Atomic Energy Research
Establishment, Bangladesh Atomic Energy Commission, Dhaka, Bangladesh

2 Institute of Energy, University of Dhaka, Dhaka, Bangladesh

3 Institute of Radiation and Polymer Technology, Atomic Energy Research
Establishment, Bangladesh Atomic Energy Commission, Dhaka, Bangladesh

4 Department of Computer Science and Engineering, Central University of Science
and Technology, Mirpur, Dhaka, Bangladesh

5 Faculty of Advanced Science and Technology, Kumamoto University, Kumamoto,
Japan

*Address all correspondence to: mosharraf22003@yahoo.com;
mosharraf22003@baec.gov.bd

† These authors contributed equally.

References

[1] M. I. Hoffert, K. Caldeira, A. K. Jain, E. F. Haites, L. D. Harvey, S. D. Potter, M. E. Schlesinger, S. H. Schneider, R. G. Watts, T. M. Wigley and D. J. Wuebbles, "Energy implications of future stabilization of atmospheric CO_2 content," Nature, vol. 395, no. 6705, pp. 881–884, 1998.

[2] F. Kabir, M. M.H. Bhuiyan and M. S. Manir, "Effect of combination of natural dyes and theblocking layer on the performance of DSSC," in Solar cells, IntechOpen, 2021.

[3] M. M.H. Bhuiyan, M. Hussain and M. A. Asgar, "Evaluation of a Solar Photovoltaic Lantern in Bangladesh Perspective," Journal of Energy & Environment, vol. 4, p. 75–82, 2005.

[4] M. M. H. Bhuiyan, M. A. Asgar, R. K. Mazumder and M. Hussain, "Economic evaluation of a stand-alone residential photovoltaic power system in Bangladesh," Renewable energy, vol. 21, no. 3–4, pp. 403–410, 2000.

[5] J. Wu, Z. Lan, S. Hao, P. Li, J. Lin, M. Huang, L. Fang and Y. Huang, "Progress on the electrolytes for dye-sensitized solar cells," Pure and Applied Chemistry, vol. 81, no. 11, pp. 2241–2258, 2008.

[6] M. M. H. Bhuiyan and M. A. Asgar, "Sizing of a stand-alone photovoltaic power system at Dhaka," Renewable Energy, vol. 28, no. 6, pp. 929–938, 2003.

[7] L. C. Andreani, A. Bozzola, P. Kowalczewski, M. Liscidini and L. Redorici, "Silicon solar cells: toward the efficiency limits," Advances in Physics: X, vol. 4, no. 1, p. 1548305.

[8] S. Ananthakumar, J. R. Kumar and S. M. Babu, "Third-Generation Solar Cells: Concept, Materials and Performance - An Overview," in Emerging

Nanostructured Materials for Energy and Environmental Science, 2019, p. 305–339.

[9] K. Kakiage, Y. Aoyama, T. Yano, K. Oya, J. I. Fujisawa and M. Hanaya, "Highly-efficient dye-sensitized solar cells with collaborative sensitization by silyl-anchor and carboxy-anchor dyes," vol. 51, no. 88, pp. 15894–15897, 2018.

[10] Dye Sensitized Solar Cells [Online]. Available from: https://gcell.com/dye-sensitized-solar-cells [Accessed 08 01 2021].

[11] D. Sengupta, P. Das, B. Mondal and K. Mukherjee, "Effects of doping, morphology and film-thickness of photo-anode," Renewable and Sustainable Energy Reviews, vol. 60, pp. 356–376, 2016.

[12] F. Kabir, S. N. Sakib, S. T. E. E. S. Uddin and M. T. F. Himel, "Enhance cell performance of DSSC by dye mixture, carbon nanotube and post TiCl4 treatment along with degradation study," Sustainable Energy Technologies and Assessments, vol. 35, pp. 298–307, 2019.

[13] J. Jaksik, H. J. Moore, T. Trad, O. I. Okoli and M. J. Uddin, "Nanostructured functional materials for advanced three-dimensional (3D) solar cells," Solar Energy Materials and Solar Cells, vol. 167, pp. 121–132, 2017.

[14] M. M.H. Bhuiyan, F. Mitsugi, T. Ueda and T. Ikegami, "Nox sensing characteristics of single wall carbon nanotube gas sensor prepared by pulsed laser ablation," International Journal of Nanomanufacturing, vol. 4, no. 1–4, pp. 186–196, 2009.

[15] F. Kabir, B. M. M. H. M. M. S. M. S. Rahaman, M. A. Khan and T. Ikegami, "Development of dye-sensitized solar

cell based on combination of natural dyes extracted from Malabar spinach and red spinach," Results in Physics, vol. 14, p. 102474, 2019.

[16] F. Kabir, M. Bhuiyan, M. R. Hossain, M. H. Bashar, M. S. Rahaman, M. S. Manir, S. M. Ullah, S. S. Uddin, M. Z.I. Mollah, R. A. Khan and S. Huque, "Improvement of efficiency of Dye Sensitized Solar Cells by optimizing the combination ratio of Natural Red and Yellow dyes," Optik, vol. 179, pp. 252–258, 2019.

[17] D. Sengupta, P. Das, U. Kasinadhuni, B. Mondal and K. Mukherjee, "Morphology induced light scattering by zinc oxide polydisperse particles: promising for dye sensitized solar cell application," Journal of Renewable and Sustainable Energy, vol. 6, no. 6, p. 063114, 2014.

[18] K. Manseki, T. Sugiura and T. Yoshida, "Microwave synthesis of size-controllable SnO2 nanocrystals for dye-sensitized solar cells," New Journal of Chemistry, vol. 38, no. 2, pp. 598–603, 2014.

[19] E. Guo and L. Yin, "Tailored SrTiO3/TiO2 heterostructures for dye-sensitized solar cells with enhanced photoelectric conversion performance," Journal of Materials Chemistry A, vol. 3, no. 25, pp. 13390–13401, 2015.

[20] Y. F. Wang, K. N. Li, Y. F. Xu, H. S. Rao, C. Y. Su and D. B. Kuang, "Hydrothermal fabrication of hierarchically macroporous Zn2SnO4 for highly efficient dye-sensitized solar cells," Nanoscale, vol. 5, no. 13, pp. 5940–5948, 2013.

[21] X. Jin, C. Liu, J. Xu, Q. Wang and D. Chen, "Size-controlled synthesis of mesoporous Nb2O5 microspheres for dye sensitized solar cells," RSC Advances, vol. 4, no. 67, pp. 35546–35553, 2014.

[22] Z. S. Wang, K. Sayama and H. Sugihara, "Efficient Eosin Y Dye-Sensitized Solar Cell Containing Br-/Br3- Electrolyte," The Journal of Physical Chemistry B, vol. 109, no. 47, pp. 22449–22455, 2005.

[23] O. Byrne, A. Coughlan, P. K. Surolia and K. R. Thampi, "Succinonitrile-based solid-state electrolytes for dyesensitised solar cells," Progress in Photovoltaics: Research and Applications, vol. 23, no. 4, pp. 417–427, 2015.

[24] P. Wang, S. M. Zakeeruddin, J. E. Moser, R. Humphry-Baker and M. Grätzel, "A Solvent-Free, SeCN−/(SeCN)3- Based Ionic Liquid Electrolyte for High-Efficiency Dye-Sensitized Nanocrystalline Solar Cells," Journal of the American Chemical Society, vol. 126, no. 23, pp. 7164–7165, 2004.

[25] N. A. Ludin, A. A.A. Mahmoud, B. M. A. A. A. H. Kadhum, and N. S.A. Karim, "Review on the development of natural dye photosensitizer for dye-sensitized solar cells," Renewable and Sustainable Energy Reviews, vol. 31, pp. 386–396, 2014.

[26] P. Avouris, J. Appenzeller, R. Martel and S. J. Wind, "Carbon Nanotube Electronics," Proceedings of the IEEE, vol. 91, no. 11, pp. 1772–1784, 2003.

[27] K. Tanaka, "Classification of Carbon," in Carbon Nanotubes and Graphene, Elsevier, 2014, pp. 1–5.

[28] T. Ueda, M. M. H. Bhuiyan, H. Norimatsu, S. Katsuki, T. Ikegami and F. Mitsugi, "Development of carbon nanotube-based gas sensors for NOx gas detection working at low temperature," Physica E: Low-dimensional Systems and Nanostructures, vol. 40, no. 7, pp. 2272–2277, 2008.

[29] P. Brown, K. Takechi and P. V. Kamat, "Single-Walled Carbon Nanotube Scaffolds for Dye-Sensitized Solar Cells," The Journal of Physical

Chemistry C, vol. 112, no. 12, pp. 4776–4782, 2008.

[30] A. Kongkanand and P. V. Kamat, "Electron storage in single wall carbon nanotubes. Fermi level equilibration in semiconductor–SWCNT suspensions," ACS nano, vol. 1, no. 1, pp. 13–21, 2007.

[31] G. H. Guai, Y. Li, C. M. Ng, C. M. Li and M. B. Chan-Park, "TiO2 Composing with Pristine, Metallic or Semiconducting Single-Walled Carbon Nanotubes: Which Gives the Best Performance for a Dye-Sensitized Solar Cell," ChemPhysChem, vol. 13, no. 10, pp. 2566–2572, 2012.

[32] C. Liu and H. M. Cheng, "Controlled growth of semiconducting and metallic single-wall carbon nanotubes," Journal of the American Chemical Society, vol. 138, no. 21, pp. 6690–6698, 2016.

[33] S. R. Jang, R. Vittal and K. J. Kim, "Incorporation of Functionalized Single-Wall Carbon Nanotubes in Dye-Sensitized TiO2 Solar Cells," Langmuir, vol. 20, no. 22, pp. 9807–9810, 2004.

[34] M. Janani, P. Srikrishnarka, S. V. Nair and A. S. Nair, "An in-depth review on the role of carbon nanostructures in dye-sensitized solar cells," Journal of Materials Chemistry A, vol. 3, no. 35, pp. 17914–17938, 2015.

[35] S. Zhang, H. Niu, Y. Lan, C. Cheng, J. Xu and X. Wang, "Synthesis of TiO2 nanoparticles on plasma-treated carbon nanotubes and its application in photoanodes of dye-sensitized solar cells," The Journal of Physical Chemistry C, vol. 115, no. 44, pp. 22025–22034, 2011.

[36] J. Yu, J. Fan and B. Cheng, "Dye-sensitized solar cells based on anatase TiO2 hollow spheres/carbon nanotube composite films," Journal of Power Sources, vol. 196, no. 18, pp. 7891–7898, 2011.

[37] S. Muduli, W. Lee, V. Dhas, S. Mujawar, M. Dubey, K. Vijayamohanan, S. H. Han and S. Ogale, "Enhanced conversion efficiency in dye-sensitized solar cells based on hydrothermally synthesized TiO2– MWCNT nanocomposites," ACS applied materials & interfaces,, vol. 1, no. 9, pp. 2030–2035, 2009.

[38] S. Sadhu and P. Poddar, "Template-Free Fabrication of Highly-Oriented Single-Crystalline 1D-Rutile TiO2-MWCNT Composite for Enhanced Photoelectrochemical Activity," The Journal of Physical Chemistry C, vol. 118, no. 33, pp. 19363–19373, 2014.

[39] Z. Peining, A. S. Nair, Y. Shengyuan, P. Shengjie, N. K. Elumalai and S. Ramakrishna, "Rice grain-shaped TiO2–CNT composite—A functional material with a novel morphology for dye-sensitized solar cells," Journal of Photochemistry and Photobiology A: Chemistr, vol. 31, no. 1, pp. 9–18, 2012.

[40] J. G. Nam, Y. J. Park, B. S. Kim and J. S. Lee, "Enhancement of the efficiency of dye-sensitized solar cell by utilizing carbon nanotube counter electrode," Scripta Materialia, vol. 62, no. 3, pp. 148–150, 2010.

[41] E. Ramasamy, W. J. Lee, D. Y. Lee and J. S. Song, "Spray coated multi-wall carbon nanotube counter electrode for tri-iodide (I3-) reduction in dye-sensitized solar cells," Electrochemistry Communications, vol. 10, no. 7, pp. 1087–1089, 2008.

[42] S. Widodo, G. Wiranto and M. N. Hidayat, "Fabrication of Dye Sensitized Solar Cells with Spray Coated Carbon Nano Tube (CNT) Based Counter Electrodes," Energy Procedia, vol. 68, no. 37–44, 2015.

[43] A. Prasetio, A. Subagio, A. Purwanto and H. Widiyandari, "Dye-sensitized solar cell based carbon

nanotube as counter electrode," in AIP Conference Proceedings, 2016.

[44] K. T. Dembele, G. S. Selopal, C. Soldano, R. Nechache, J. C. Rimada, I. Concina, G. Sberveglieri, F. Rosei and A. Vomiero, "Hybrid carbon nanotubes–TiO2 photoanodes for high efficiency dye-sensitized solar cells," The Journal of Physical Chemistry C, vol. 117, no. 28, pp. 14510–14517, 2013.

[45] F. Kabir, S. N. Sakib and S. S. Uddin, "Effect of MWCNT's concentration in TiO2 based DSSC and degradation study of the cell," Journal of Renewable and Sustainable Energy, vol. 11, no. 2, p. 023502, 2019.

[46] I. Ahmad, U. Khan and K. Gun'ko, "Graphene, carbon nanotube and ionic liquid mixtures: towards new quasi-solid state electrolytes for dye sensitised solar cells," Journal of Materials Chemistry, vol. 21, no. 42, pp. 16990–16996, 2011.

[47] H. C. Lee, M. S. Akhtar, J. G. Park, K. J. Kim, S. K. Lee and O. Yang, "Carbon Nanotube (CNT)–Polymethyl Methacrylate (PMMA) Composite Electrolyte for Solid-State Dye Sensitized Solar Cells," Journal of nanoscience and nanotechnology, vol. 10, no. 5, pp. 3502–3507, 2010.

[48] Y. Xiao, J. Wu, G. Yue, J. Lin, M. Huang and Z. Lan, "Low temperature preparation of a high performance Pt/SWCNT counter electrode for flexible dye-sensitized solar cells," Electrochimica Acta, vol. 56, no. 24, pp. 8545–8550, 2011.

[49] A. Kongkanand, R. Martínez Domínguez and P. V. Kamat, "Single wall carbon nanotube scaffolds for photoelectrochemical solar cells. Capture and transport of photogenerated electrons," Nano letters, vol. 7, no. 3, pp. 676–680, 2007.

[50] S. Zhang, C. Ji, Z. Bian, R. Liu, X. Xia, D. Yun, L. Zhang, C. Huang and A. Cao, "Single-Wire Dye-Sensitized Solar Cells Wrapped by Carbon Nanotube Film Electrodes," Nano letters, vol. 11, no. 8, pp. 3383–3387, 2011.

[51] Z. Yang, J. Deng, X. Sun, H. Li and H. Peng, "Stretchable, wearable dye-sensitized solar cells," Advanced Materials, vol. 26, no. 17, pp. 2643–2647, 2014.